

Identification of Causative Factors of Seismotectonic Activities in Kwoi and Mpape Using Aeromagnetic Data

Ebi Solomon ^{1,*}, Nwankwo Cyril Ngozi ², Nwosu Leo ², Daomi Esau Abiodun ¹, Garba Bashir Abdullahi ¹ and Abdulhadi Muzaffar Lawan ³

¹ National Space Research and Development Agency, Centre for Geodesy and Geodynamics, Toro, Bauchi State, Nigeria.

² Department of Physics, University of Port Harcourt, Port Harcourt, Nigeria.

³ National Space Research and Development Agency, Zonal Advance Space Technology Application Laboratory, Kano State, Nigeria.

World Journal of Advanced Research and Reviews, 2026, 30(02), 812-829

Publication history: Received on 02 April 2026; revised on 08 May 2026; accepted on 11 May 2026

Article DOI: <https://doi.org/10.30574/wjarr.2026.30.2.1290>

Abstract

An aeromagnetic reconnaissance study is adopted to delineate the subsurface structures of the seismotectonic activities on 11th-12th September, 2016 at Kwoi, Kaduna State, northwestern Nigeria and on the 5th-7th September, 2018 at Mpape, Federal Capital Territory, Abuja, northcentral Nigeria. The map was processed using Geosoft Oasis Montaj software version 6.4.2. Data enhancement techniques were carried out and interpreted to ascertain the causative factors of recent earthquakes in Nigeria. Analysis on the TMI map shows both positive and negative anomalies ranging from -48 nT to 88 nT. The high magnetic susceptibilities are prominent around the central, southern, southwestern and northeastern parts of the study area, which correspond to Kwoi and Mpape. The intensity of the RTE map ranges from -29 nT to 73 nT, with high-intensity magnetic response trending NE-SW direction, and low-intensity striking NW-SE direction. The FVD map is characterized by anomaly gradient values ranging from -0.5 nT/km to 0.03 nT/km. Linearments shown by the FVD, TDR, and Upward Continuation maps are continuous, discontinuous and deep seated. The long linear features represent major fault lines on the map cutting across Kwoi and Mpape, trending NE-SW and SE-NW direction, which coincides with the regional North Atlantic Romanche fault system. The study's findings have provided significant insights into the subsurface structural architecture of seismotectonic activities within Kwoi and Mpape northwestern and northcentral Nigeria.

Keyword: Seismotectonic; Subsurface structures; Aeromagnetic; Kwoi; Mpape

1. Introduction

The seismicity of Nigeria has always been known as low to medium. Going by the increasing occurrence of seismic events in the country over the last few decades and the alarming damages now manifestly associated with some events in Nigeria, the country is gradually transiting into one of the regions with frequent earthquakes. (Osagie, 2008; Akpan and Yakubu, 2010). An earthquake of moderate size occurred in the investigation areas on September 11th and 12th, 2016 (Kwoi earthquake) and September 5th-7th, 2018 (Mpape earthquake), with a Modified Mercalli intensity (MMI) of III for the Kwoi event and a magnitude of 2.6-3.0 for the Mpape event (CGG, 2018). Earth tremors have been felt in the country over time, particularly in the south-western and north-western region with the recent event in north-central Nigeria; locations that have felt vibrations as a result of previous tremors include Lagos, Ibadan, and Ile-Ife in 1939 (Ananaba, 1991; Oluwafemi et al., 2018), Ijebu-Ode in 1963 (Ajakaiya et al., 1987), Ibadan, Ijebu-Ode, Shagamu, and Abeokuta in 1984 (Ojo, 1995), Ibadan and Ijebu-Ode in 1990 (Osagie, 2008; Akpan and Yakubu, 2010; Ojo, 1995), Okitipupa in 1997; Okitipupa, Ibadan, Ijebu-Ode, Akure, Shagamu, Abeokuta, and Oyo in 2000 (Akpan and Yakubu, 2010;

* Corresponding author: Ebi S

Elueza, 2003). Abomey-Calavi in 2009; Kwoi in 2016; Saki in 2016; Igbogene in 2016; and Mpape in 2018 (CGG, 2018; Isogun et al., 2018; Adepelumi, 2019; Ebi et al., 2020; Umeaku and Emujakporue, 2020).

The reoccurrence of earth tremor within the country has necessitated the careful monitoring of seismic activities, which have shown to be possible hazards in Nigeria. There is a need to carefully monitor those activities in Nigeria that have the potential to cause the tremors by conducting a detailed investigation of the cause of the tremors using a geophysical technique to identify the major fault zones and other features that are responsible for the tremors using the magnetic method. The magnetic method is a geophysical survey approach that uses variations in the magnetic properties of minerals to delineate the earth's subsurface. According to Telford et al. (1990), the method necessitates the acquisition and measurement of variations in the Earth's magnetic field that result from changes in the near-surface rocks' magnetic characteristics or variations in the subsurface geological structure.

However, some researchers have carried out various studies within the basement complex on the possible causes of earthquakes in the country using various geophysical techniques to identify and delineate subsurface structures within areas that have experienced earthquakes (Sykes, 1978; Anifowose et al., 2010; Tshala et al., 2015). The geological characteristics where the studies were carried out are described by their structural features, petrology, potential for mineralization, hydrogeology, and geochemical properties.

Murat (1988) obtained that the major cause of earth tremor within the basement complex is as a result of principal stress acting WNW-ESE, their findings correspond with the regional stress models proposed by Adepelumi et al. (2008), Nwankwoala and Orji (2018), and Eze et al. (2011). Adepelumi et al. (2008) attribute the major causes of earth tremors in the southwestern part of the country is the Ifewara transcurrent fault. Their founding was obtained by integrated geophysical techniques using dipole-dipole resistivity (DDR) and magnetic in delineating the Ifewara transcurrent fault, which they discovered is trending in a NNE-SSW direction, with a magnetic anomaly breadth ranging from 90-150 metres, its dip angle ranging between 75° and 85°, and its thickness being roughly 15 metres. Eze et al. (2011), in their study on "Mechanical Model for Nigerian Intraplate Earth Tremors," examined a total of 15 recorded seismic events in Nigeria in order to ascertain possible causes of these tremors. One of the potential causes of the intraplate tremors was reported to be a regional stress created between the Congo Craton and the West African Craton, with an inferred primary stress acting West Northwest-East Southeast. They also suggested that various degrees of seismicity throughout the nation may be caused by inhomogeneities and zones of weakness in the crust as a result of previous magmatic intrusions and other tectonic processes, Nwankwoala and Orji (2018) and Tsalha et al. (2015) agreed with the result obtained by Eze et al. (2011).

In order to comprehend the seismotectonic activity in southwest Nigeria, Akpan et al. (2014) examined the earth tremor that happened on September 11, 2009, and its implications. They concluded that the earthquake was a reactivation of a hidden high-angle fault in the Precambrian basement, which is indicated by currently observed NE-SW trends, linking the seismic activity of the region to the Atlantic fracture zones. Onuoha (1988) had a contrary view; he said that the origins of earth tremors within the nation were not the fracture zones stretching from the Atlantic Ocean but rather zones of weakness and regional stress in the crust or the transfer of stress from the plate. In their preliminary geological evidence for multiple tremors in Kwoi, north-central Nigeria, Nathaniel et al. (2020) used seismic data, aeromagnetic data, and Digital Terrain Model (DTM) for structural mapping to determine the pattern and intensity of cracks on nearby structures, rocks, and hanging walls of slopes. According to their study findings, the major evidence that proved a possible link to the area of highest impact was the tremor-triggered displacement of a 4 by 3 m diameter rock boulder located about a kilometre from Kwoi town, about 3 km from the nearest epicentre, that fell through an average distance of 25 m, separating the fresh granite boulder into two and causing a high impact scar on its path. Residents of Kwoi and its surroundings were struck by seismic vibrations, which emanated and propagated laterally from the rocks along a northwest-southeast profile, with the epicenters plotted along a predicted trend that aligns with the Chain Fracture Zone of the North Atlantic. High-resolution aeromagnetic data was used by Ukeaku and Emujakporue (2020) and Oyibo et al. (2022) to evaluate the geophysical and geological structural features of the 2016 earth quake area in parts of Kaduna State, northwestern Nigeria. Based on their findings, structural trends indicating the tectonics of the studied area were delineated to strike in the NE-SE, N-S, E-W, NNW-SSE, and NNE-SSW directions. These tectonic trends could be an indicator that magnetism or metamorphisms are responsible for tectonic deformations in the study area. The Pan African Orogeny were presumed to be the structural trends existing within the area in the NNE-SSW and NNW-SSE directions. The tremors' spark mechanism is linked to the NW-SW and NE-SW tectonic trends, which represent a possible shear zone extending from the regional North Atlantic Romanche fault system to Nigeria's Precambrian basement, which is referred to as the main seismic energy source that generates earth tremors within north-central Nigeria.

This study has been able to delineate subsurface structures of Kwoi and Mpape region by producing detail structural maps, delineating lithologic boundaries, and estimating the depth of the faults within the study region.

2. Location and Geology of the Study Area

The study areas are located at Kwoi, Kaduna State (north-western) Nigeria, and Mpape, Abuja (Federal Capital Territory), north-central Nigeria, between latitudes $9^{\circ} 14'N$ - $9^{\circ} 57'N$ and Longitudes $7^{\circ} 60'E$ - $8^{\circ} 07'E$. Kwoi is a town in the Jaba local government area and the capital of the Ham (Jaba) chiefdom in southern Kaduna (Figure 1). Mpape is a major and densely populated district in Abuja, the Federal Capital Territory. It is situated opposite Maitama main across the highway connecting Kubwa and Asokoro, Katampe to the south-west, and Maitama 2 or Maitama extension to the north. Mpape is one of the districts under the Bwari Area Council.

The Abuja-Kwoi region is located in the Basement Complex of Central Nigeria, which is underlain by Precambrian rocks with the major lithological units such as Amphibolite-Schists/Amphibolites, Biotite-granites, Quartzites/Quartzite-Schists, and Migmatite-gneiss (Figure 2), all of which are intruded by Pan African Older Granite rocks (Ajibade, 1976; Ajibade and Woakes, 1983; and Obaje, 2009). These Basement complex rocks are classified as follows: The migmatitic-gneiss complex (MGC), or the older metasediments; the metasediments, or Schist belts; and the older granites (Oyawoye, 1964 and 1965). According to Rahman and Dada (1988 and 2006), magmatites-gneiss is regarded as the "senso stricto" of the basement. They are the most predominant rock, which covers about half of the Nigerian basement complex (Kröner et al., 2001). It is a diverse collection of rocks that includes metamorphosed basic and ultrabasic rocks, banded gneisses, and migmatized gneisses (Rahaman, 1988). These basement rocks' foliation generally follows a NE-SW trend, with sporadic E-W foliation. The rocks' gradational contacts with high-grade metamorphic rocks indicate that granitization was likely their mode of formation (Obiora, 2005). The metasediments, which are split into "ancient metasediments/older metasediments" and "newer metasediments/younger metasediments," have been identified as discontinuous north-south trending belts inside the basement complex of ancient Pre-cambrian sedimentary and volcanic rocks. (Oyawoye, 1972; McCurry, 1976). The older metasediments were formed about 2,500 Ma. They are high-grade metasedimentary remnants in gneisses and migmatites, made up of Arkosic quartzite, Calc-silicate rocks, and high-grade Schist, and they can be found as lensoid remnants in regional gneisses or as paleosomes in migmatites. Younger metasediments are dominated by schist groups with low-grade sediment mostly made up of quartzite, metaconglomerate, marble, pelitic and semipelitic schist, mafic to ultramafic rocks, calc-silicate rock, acid to intermediate volcanic rocks, and banded iron formations (McCurry, 1976; Danbatta, 2008). The Older Granites, also referred to as the Pan-African Granitoids, are syn-to late-tectonic intrusions into the "MGC" and the Schist belts. They range in size from small sub-circular stocks to large batholiths (Fitches et al., 1985; Wright et al., 1985). They are often weakly foliated and expressed as foliated granites and gneissic granites.

The structural characteristics found in the research area include faults and magnetic data lineaments. A number of the fault lines on the map were delineated to be deep-seated in origin and old in age and have developed as a result of thermotectonic deformational processes, especially during the Pan-African Orogeny.

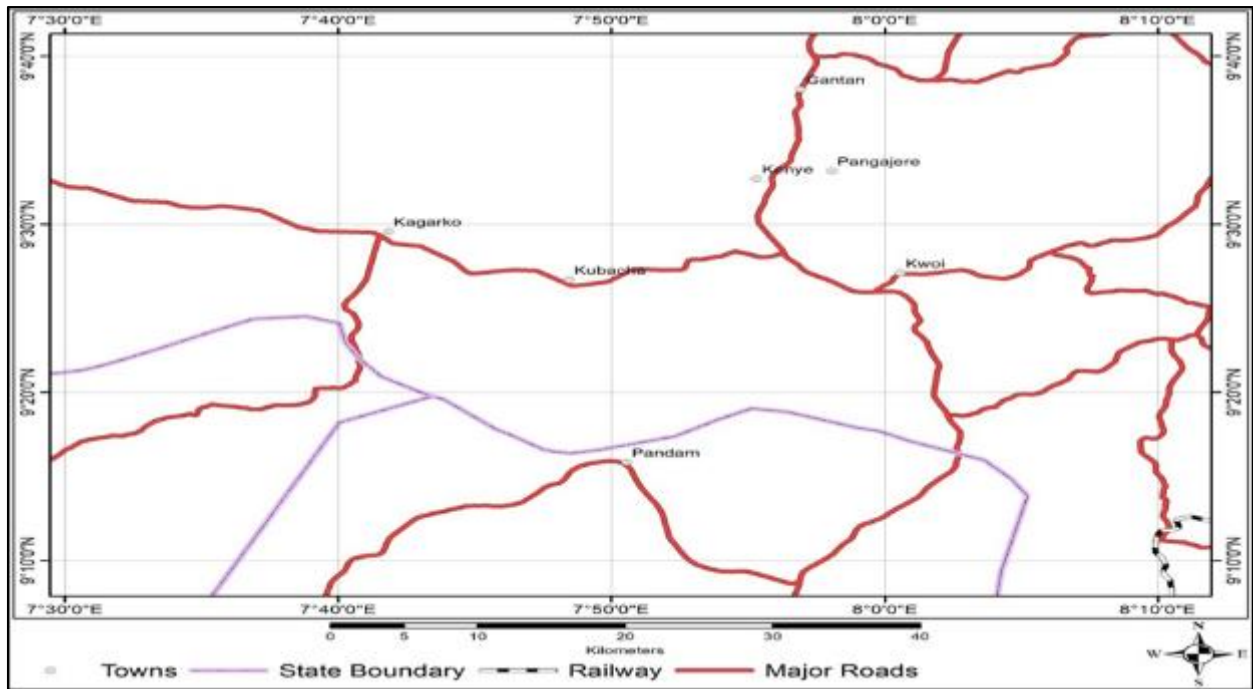


Figure 1 Location Map of the Study

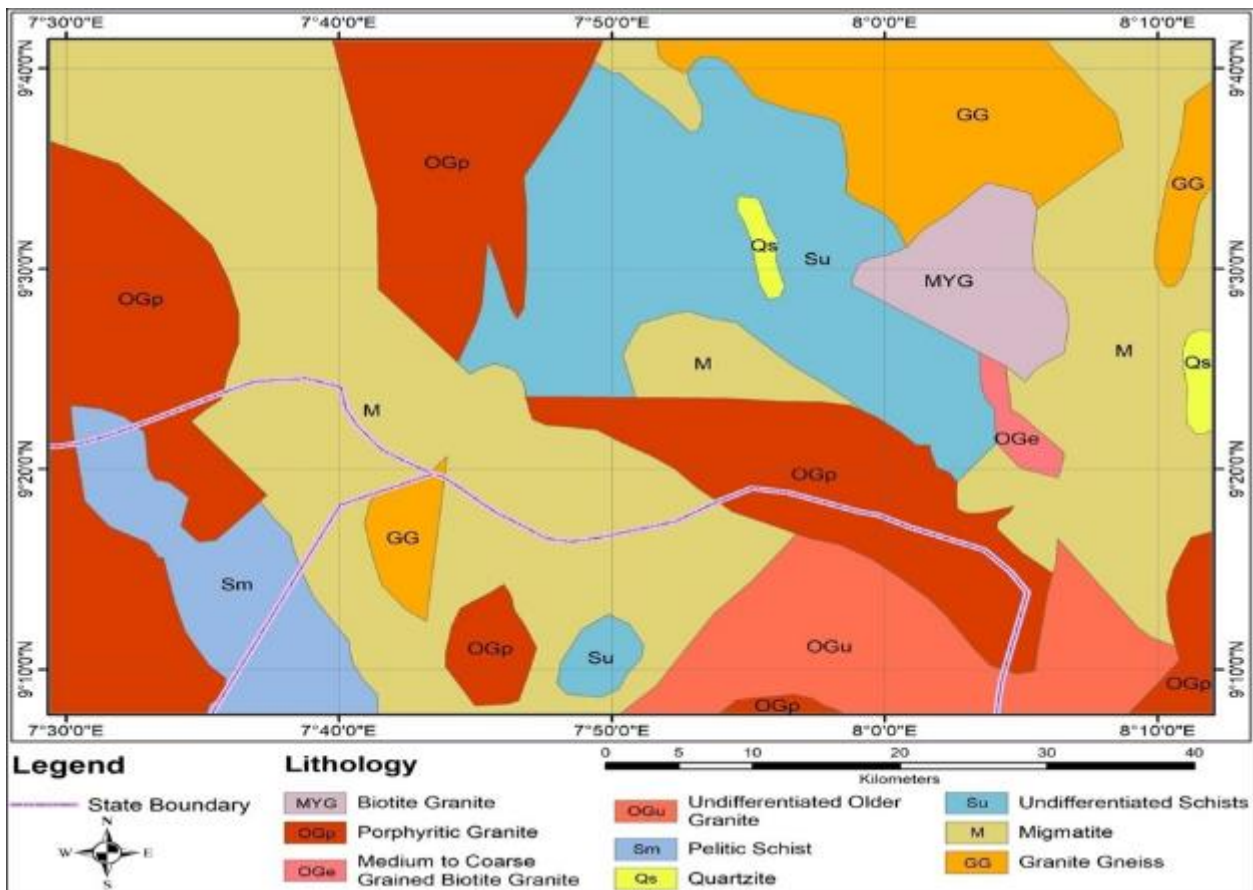


Figure 2 Geology Map of the Study Area

3. Material and Methods

The subsurface magnetic anomaly structures of nine digitized high-resolution aeromagnetic data of sheets 165, 166, 167, 186, 187, 188, 207, 208 and 209, was obtained from the Nigeria Geological Survey Agency (NGSA), and the maps were processed, analyzed, and interpreted. During the processing, various data enhancement techniques were carried out and interpreted. Software such as Geosoft® Oasis Montaj™ software and Surfer was used to analyze and interpret the aeromagnetic data.

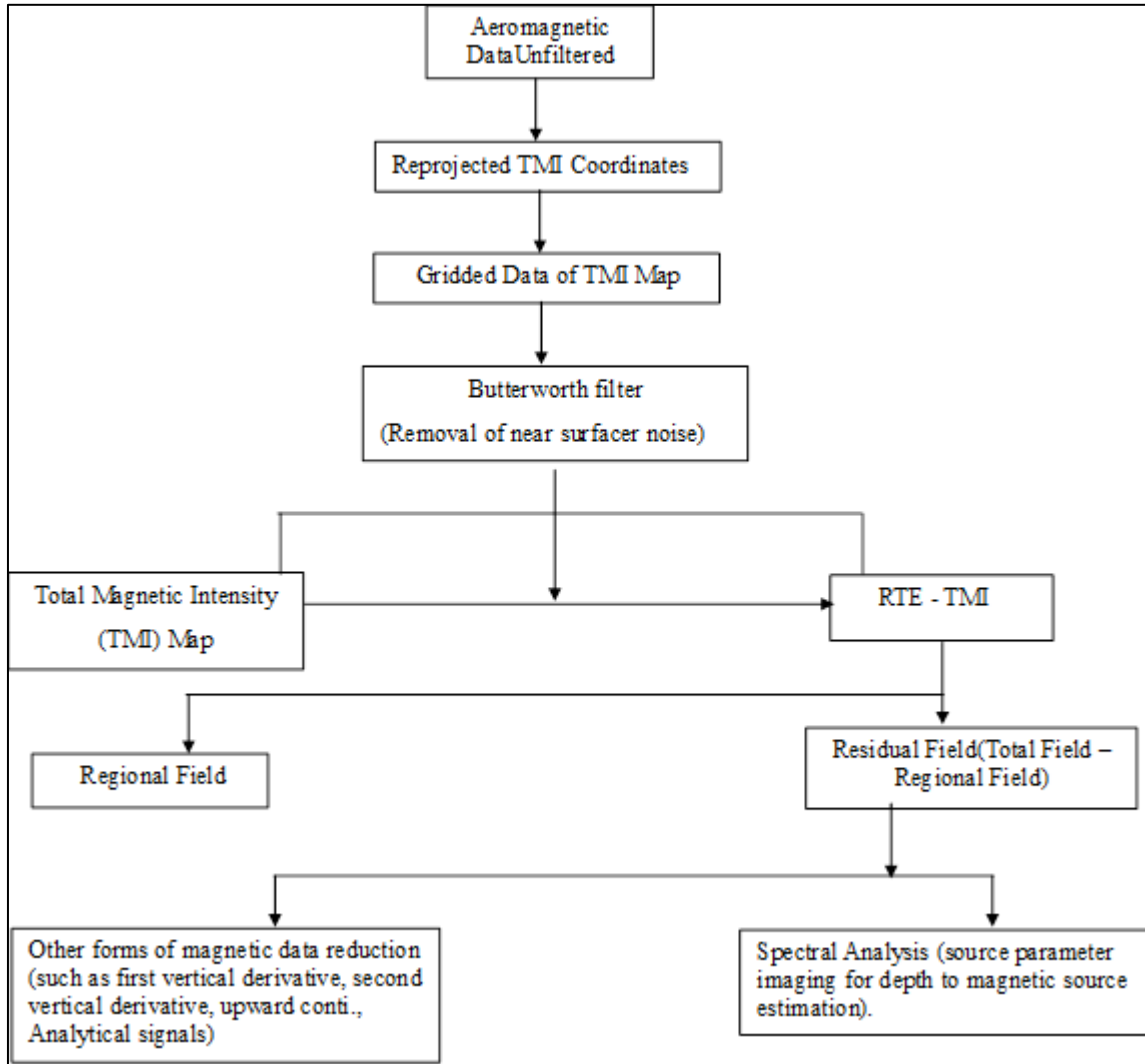


Figure 3 Workflow for application of aeromagnetic survey to geophysical methods

3.1. Total Magnetic Intensity (TMI)

The TMI grid is the interpreter's primary data, which is presented as the corrected survey measurements and serves as an important reference point while interpreting the filtered and transformed data.

3.2. Reduction to Magnetic Equator (RTE)

The RTE-TMI image was generated using the Reduction to Magnetic Equator (RTE) filter, which was used to centre structures and anomalous bodies over their actual positions. Anomalies are caused by the inclination and declination of the body's magnetization, the inclination and declination of the local earth's field, and the body's orientation with regard to the magnetic north. (Blakely, 1995).

3.3. First Vertical Derivative (FVD)

This derivative transformation was performed on the aeromagnetic residual data in order to sharpen the edges of anomalies as well as other distinctive features (Feumoe et al., 2012; Cooper, 1997). This transformation or filtering technique accentuates the high wave number section at the expense of the low wave number part. The algorithm is described by (Gunn, 1975) as follows:

$$M(x, y) = M(x, y) \sqrt{[(x^2 + y^2)/n]^n} \quad 1$$

where n is the order of the derivative.

3.4. Second Vertical Derivative (SVD)

Unwanted sources were suppressed using SVD filtering when they were concealed by a larger regional trend. In this situation, it emphasises short-wavelength components, which sharpen the edges of the observed anomalies; it also tends to decrease the complexity of the anomalies and allows for a clearer contrast between the minor trends and lineaments or faults that are responsible for the larger anomalies (Faboye et al., 2003).

3.5. Upward Continuation (UC)

This is a mathematical technique that projects potential field data from one elevation to a higher elevation. By projecting to a higher plane, we are decreasing the influence of the local (residual) anomaly while enhancing the regional effects; these effects are obtained by smoothing out the short wavelength. The anomalies have an attenuated effect with regard to wavelength; the shorter the wavelength, the greater the degree of attenuation (Mekonnen, 2004).

The upward continued ΔF (the total field magnetic anomaly) at higher level ($z = -h$) is expressed as,

$$\Delta F(x, y, -h) = \frac{h}{2\pi} \iint \frac{\Delta F(x, y, 0) dx dy}{[(x-x_0)^2 + (y-y_0)^2 + h^2]^{\frac{3}{2}}} \quad 2$$

where $\Delta F(x, y, -h)$ = Total field at the point above the surface on which

$F(x, y, 0)$ is known, h = elevation above the surface (Telford et al., 1990).

3.6. Tilt-angle Derivative (TDR)

The Tilt Derivative (TDR) is generated using the tilt derivative filter. Using the theory that the zero contours are the boundaries of the formation equation, it is used to identify structures, trends, contacts, and edges or boundaries of magnetic sources. It is also used to enhance both weak and strong magnetic anomalies of the region by positioning an anomaly over its source, especially at shallow depths.

$$HD_TDR = \sqrt{\frac{dT}{dx} + \frac{dT}{dy}} \quad 3$$

$$TDR = \arctan(1VDT/HD_TDR) \quad 4$$

where; $1VDT$ denotes the first vertical derivative in z -direction, dT/dx represent the derivative in x -direction and dT/dy represent the derivative in y -direction.

3.7. Analytic Signal (ASG)

Analytic Signal (ASG), also known as total gradient, is generated by the horizontal and vertical gradient in conjunction with magnetic anomalies, and the resulting signal is applied in both the space and frequency domains, producing a maximum that passes through separate objects as well as their edges

Nabighian (1972) first established the amplitude of an analytical signal in two dimensions, which he subsequently expanded to three dimensions (Nabighian, 1984; Roest et al., 1992). The two dimensions (2D) are primarily used as a tool for depth estimation and position of sources, while the three dimensional (3D) are used both as mapping tool and depth-to-source technique which gives an in-depth understanding about the nature of causative magnetization.

For 2D or 3D bodies, respectively, the two or three orthogonal derivatives of the field are used to compute the amplitude A of the ASG of the entire magnetic field F .

Mathematically, the ASG of potential field data in 2-D is expressed as,

$$A(x) = \varphi_x + i\varphi_z \tag{5}$$

Where the potential field's 2D analytical signal amplitude is

$$|A(x)| = \sqrt{\varphi_x^2 + \varphi_z^2} \tag{6}$$

Roest et al. (1992) represent the analytic signal in three dimensions as a vector including the horizontal derivatives with their Hilbert transform, as well as the three-dimensional analytical amplitude of the potential field $\phi(x, y)$ recorded on a horizontal plane.

$$|A(x, y)| = \sqrt{\varphi_x^2 + \varphi_y^2 + \varphi_z^2} \tag{7}$$

The analytic signal for 3D is expressed as:

$$A(x, y, z) = \frac{\partial \Delta F}{\partial x} i + \frac{\partial \Delta F}{\partial y} j + i \frac{\partial \Delta F}{\partial z} k \tag{8}$$

The amplitudes (A) of the ASG of magnetic is express in equation (9) as the square root of the squared sum of the vertical and horizontal derivatives of the magnetic field (Nabighian, 1972).

$$ASG = |A(x, y)| = \sqrt{\left(\frac{\partial \Delta F}{\partial x}\right)^2 + \left(\frac{\partial \Delta F}{\partial y}\right)^2 + \left(\frac{\partial \Delta F}{\partial z}\right)^2} \tag{9}$$

The real and imaginary components that make up the Fourier transform of equation (8) represent the horizontal and vertical derivatives for ΔF , respectively.

3.8. Source Parameter Imaging (SPI)

Source Parameter Imaging is a powerful, simple, and fast technique for source location and basement depth calculation of magnetic sources using the relationship between local wave number (k) and source depth from an analytical signal of the observed field, which may be obtained at any point within a data grid through horizontal and vertical gradients.

SPI is similar to deconvolution. Tests on real data sets using drill hole control have shown that the accuracy of results from SPI is approximately +/- 20% (Salako, 2014; Al-Badani and Al-Wathaf, 2018). The advantage of SPI is that it generates a more comprehensive set of coherent solutions that can be easily interpreted (Thurston and Smith, 1997). According to Nabighian (1972), the analytical signal $A(x, z)$ is defined as:

$$A(x, z) = \frac{\partial M(x, y)}{\partial x} j \frac{\partial M(x, z)}{\partial z} \tag{10}$$

where $M(x, z)$ denotes the magnitude of the anomalous total magnetic field, j denotes the imaginary number, and z and x represent Cartesian coordinates describing the vertical and horizontal directions, respectively.

Nabighian (1972) established that the horizontal and vertical derivatives, including the real and imaginary parts of a 2D analytical signal, are Hilbert transformation pairs given by

$$\frac{\partial M(x, z)}{\partial x} \Leftrightarrow \frac{\partial M(x, z)}{\partial z} \tag{11}$$

Where \Leftrightarrow represent the transformation pair.

The local wave number K (in radians per ground unit) for this analytical signal is defined by Thurston and Smith (1997) as

$$K = 2\pi f_0 \tag{12}$$

$$f_0 = \frac{1}{2\pi} \frac{\partial}{\partial x} \tan^{-1} \left[\frac{\frac{\partial M(x,z)}{\partial z}}{\frac{\partial M(x,z)}{\partial x}} \right] \tag{13}$$

where f_0 is cycles/ground unit and K is the wave number in radian per ground unit

$$K = \frac{\partial}{\partial x} \tan^{-1} \left[\frac{\frac{\partial M(x,z)}{\partial z}}{\frac{\partial M(x,z)}{\partial x}} \right] \tag{14}$$

Nabighian (1972) derives the mathematical equation for the vertical and horizontal gradient of a sloping contact model as:

$$\frac{\partial M(x,z)}{\partial x} = \frac{2xMcsin\beta.xcos(21-\beta-90^0)-hsin(21-\beta-90^0)}{h^2+x^2} \tag{15}$$

and

$$\frac{\partial M(x,z)}{\partial x} = \frac{2xMcsin\beta.hcos(21-\beta-90^0)-xsin(21-\beta-90^0)}{h^2+x^2} \tag{16}$$

where x denotes susceptibility contrast that exists at the contact, M denote magnitude of the earth's magnetic field (the inducing field), $c = 1 - \cos^2 i \sin^2 \alpha$, α denote angle between the positive x-axis and magnetic north, i denote ambient-field inclination, $\tan i = \sin i / \cos i$, β denote the dip (measured from the positive x-axis), h is the depth to the top of the contact and all trigonometric evidence is expressed in degrees.

The origin of the profile line ($x = 0$) is situated directly over the edge due to the way the coordinate system has been set up. The wave number for a contact profile is given by substituting equations 15 and 16 into equation 14 as follows:

$$k_{max} = \frac{1}{h} \tag{17}$$

and

$$Depth (h) = 1/k_{max} \tag{18}$$

where K_{max} denotes the analytical signal wave number

h denotes the depth to the point of contact.

A second wave number can also be produced by applying the concept of Hsu et al. (1996) to an analytical signal made up of second-order derivatives of the total field.

The wave number is certainly unaffected by the susceptibility contrast, the source's dip, inclination, declination, and the earth's magnetic field strength, which is illustrated by equation 15. The SPI technique is based on Equation 10 (Adetona and Abu, 2013). It makes use of the relationship involving the source depth and local wave number of the measured field, which may be estimated for each location within a data grid using horizontal and vertical gradients (Thurston and Smith, 1997). The peaks of local wave numbers for vertical contacts define the inverse of depth. An image representing the depth is shown (in aggregated colour). The source-parameter grids' image processing improves detail and produces maps that are easier for non-professionals to understand (Ojoh, 1992).

4. Result and Discussion

Results of qualitative analysis on the aeromagnetic data are presented in figure 4 - 15.

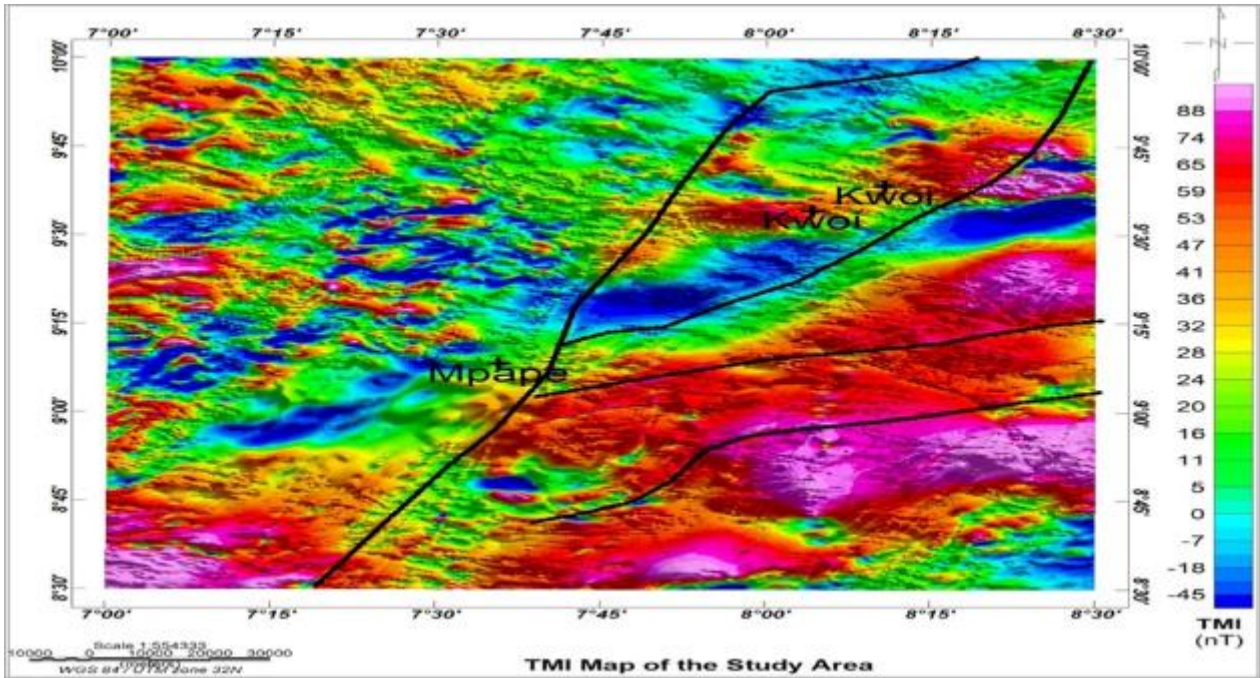


Figure 4 Total Magnetic Intensity Map (TMI)

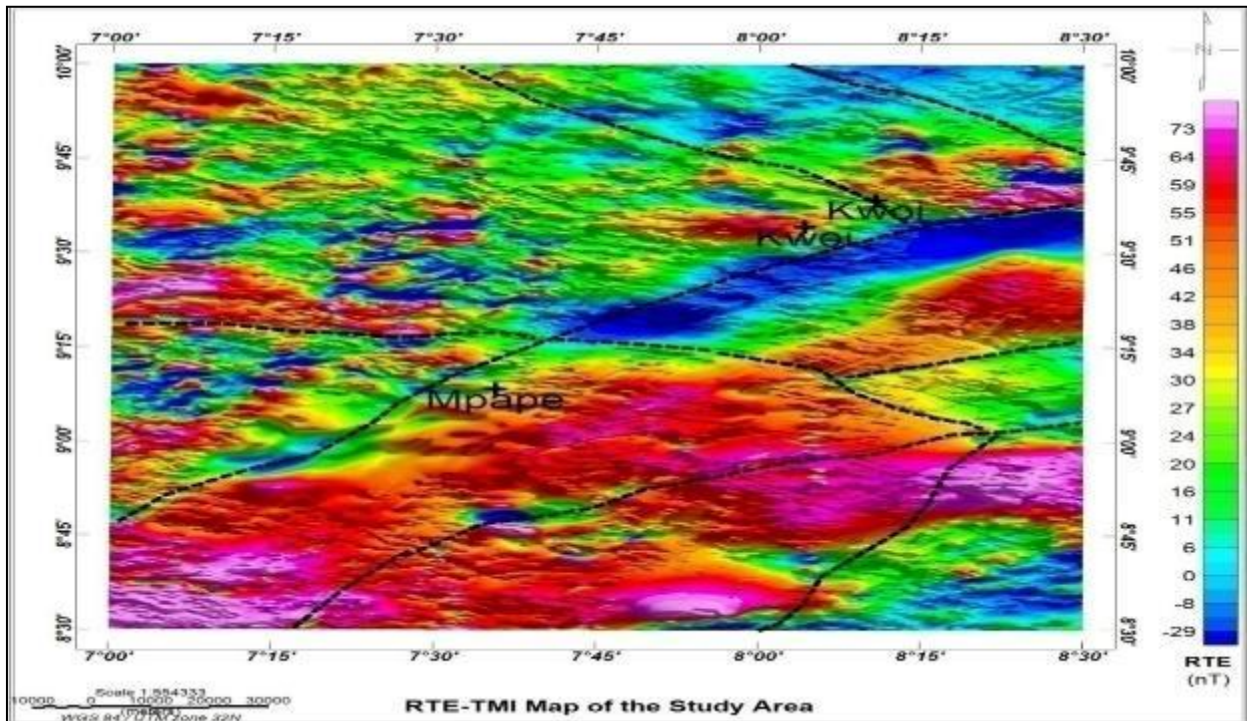


Figure 5 Reduction to Equator (RTE) Map From TMI

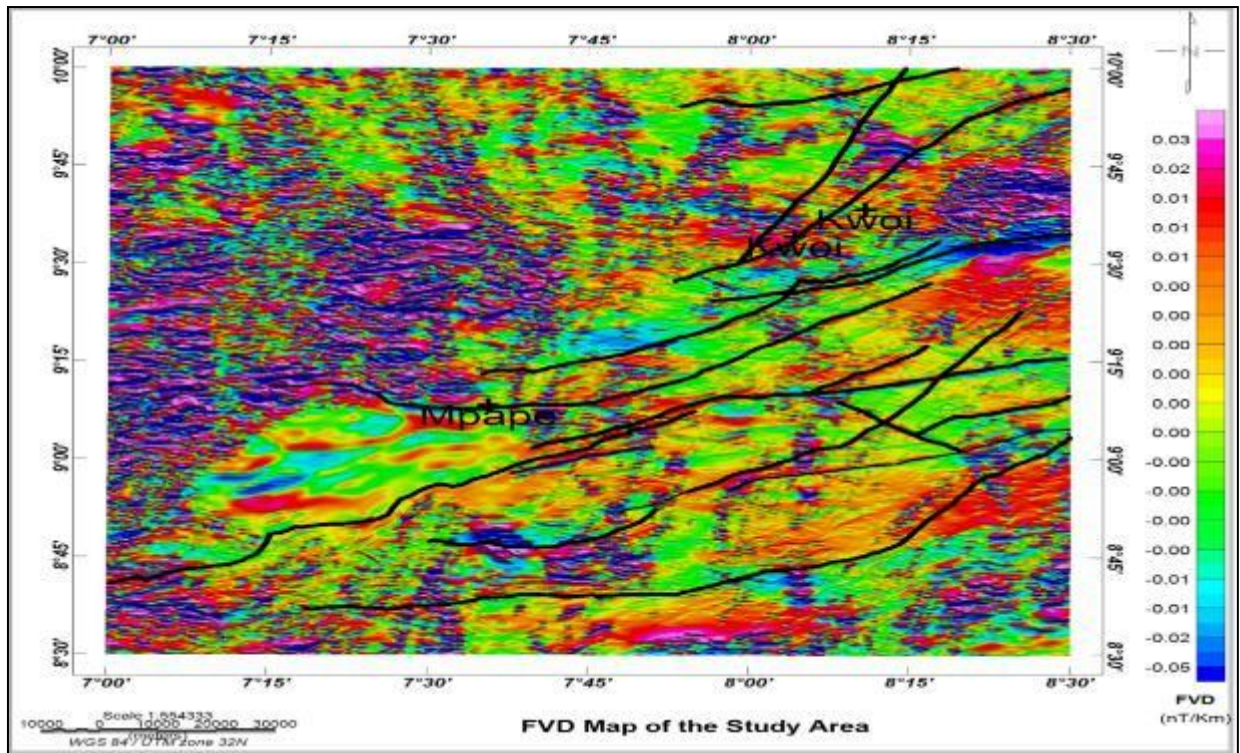


Figure 6 First Vertical Derivative of TMI Reduced to Equator Map

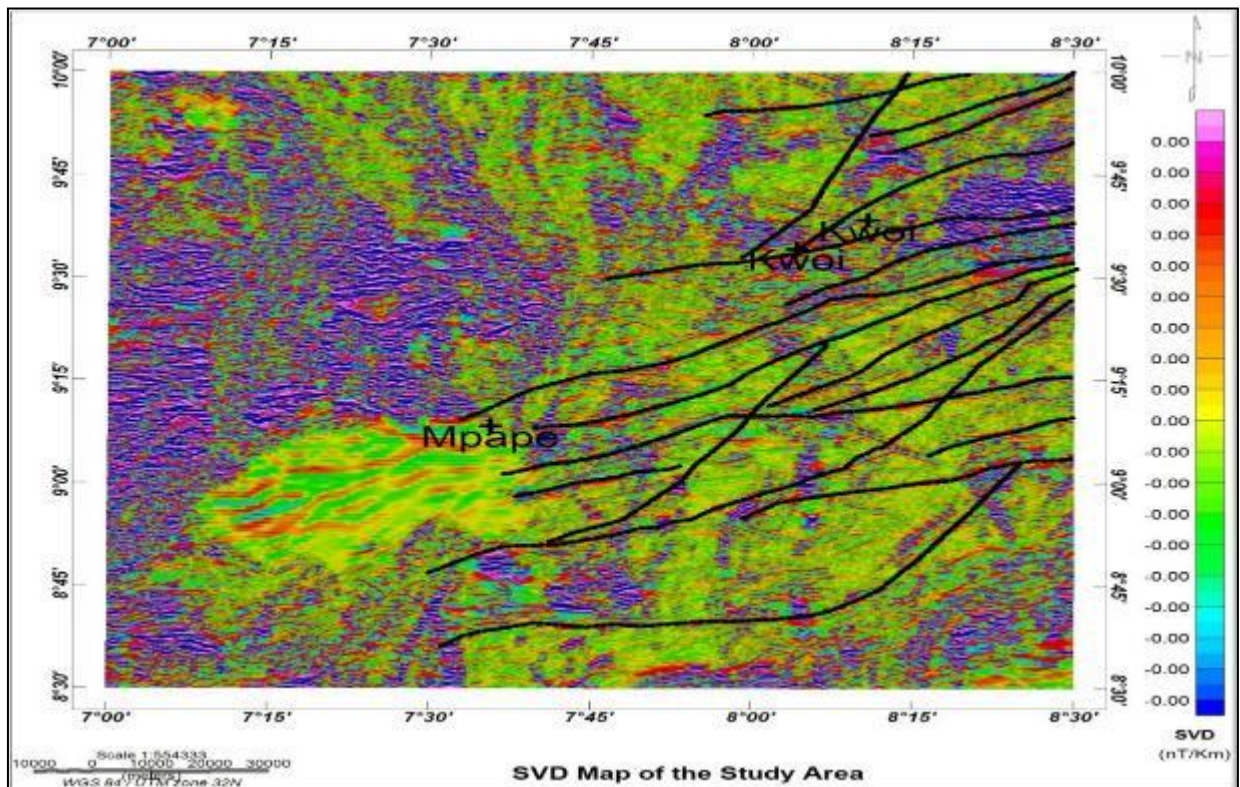


Figure 7 Second Vertical Derivative Map

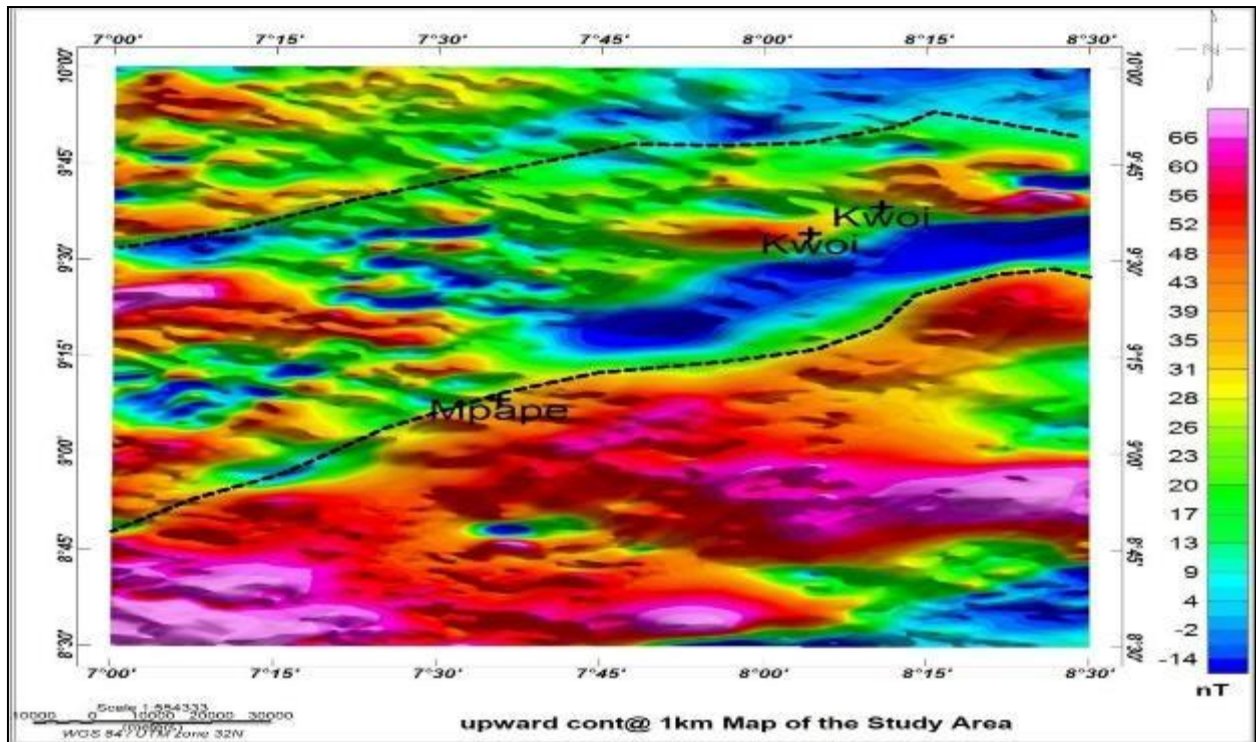


Figure 8 Upward Continuation Map at 1 km

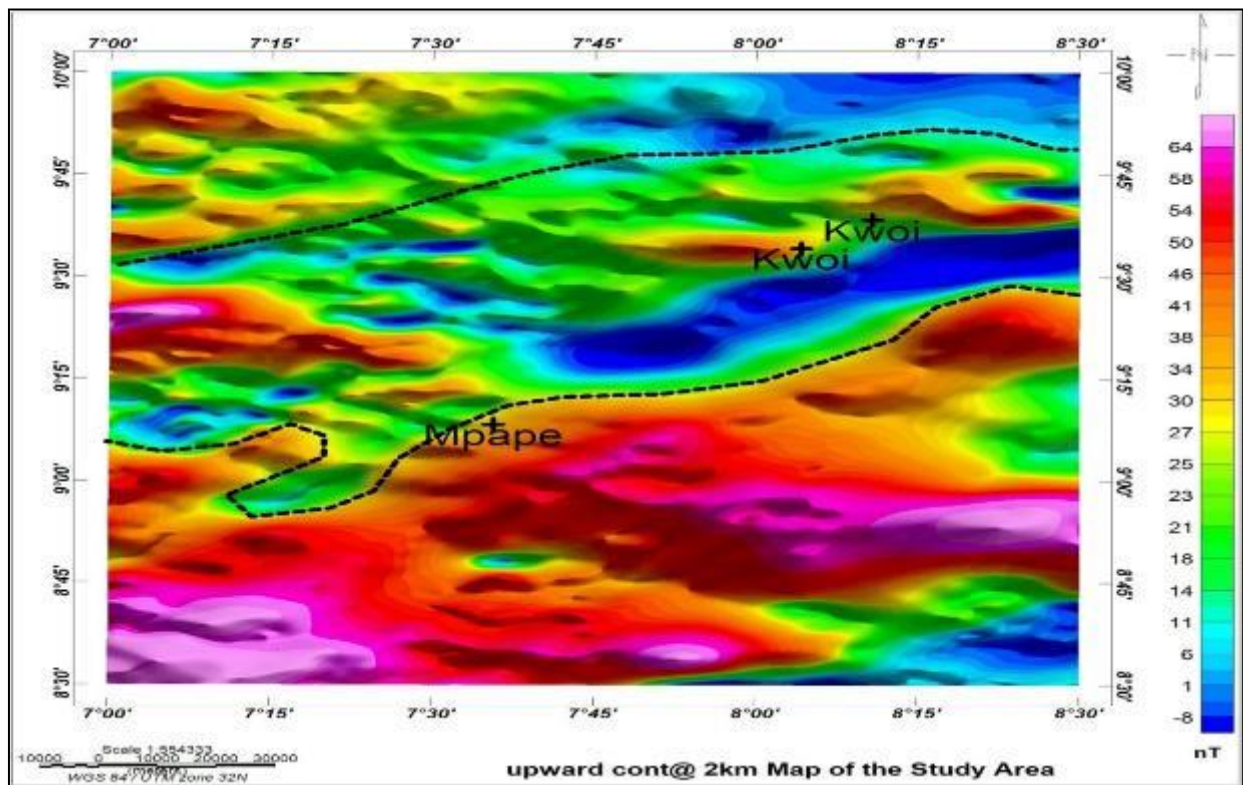


Figure 9 Upward Continuation Map at 2 km

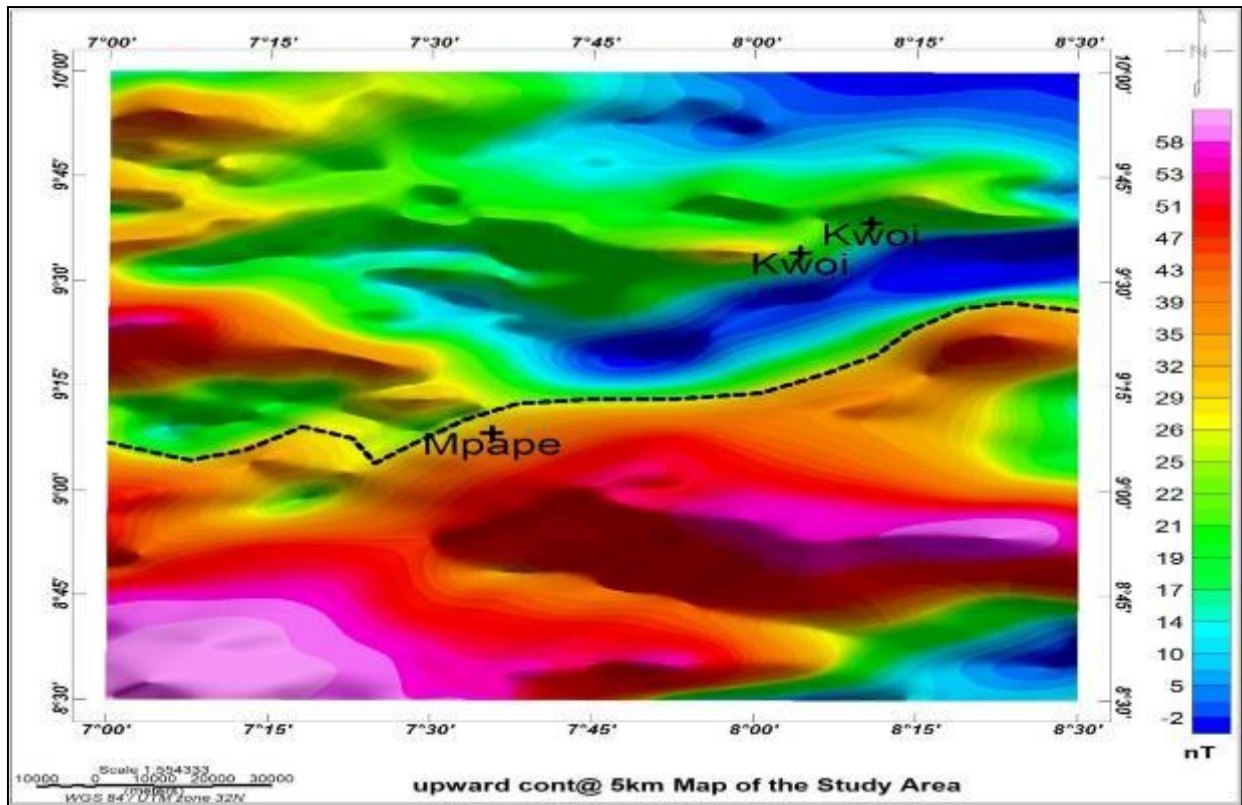


Figure 10 Upward Continuation Map at 5 km

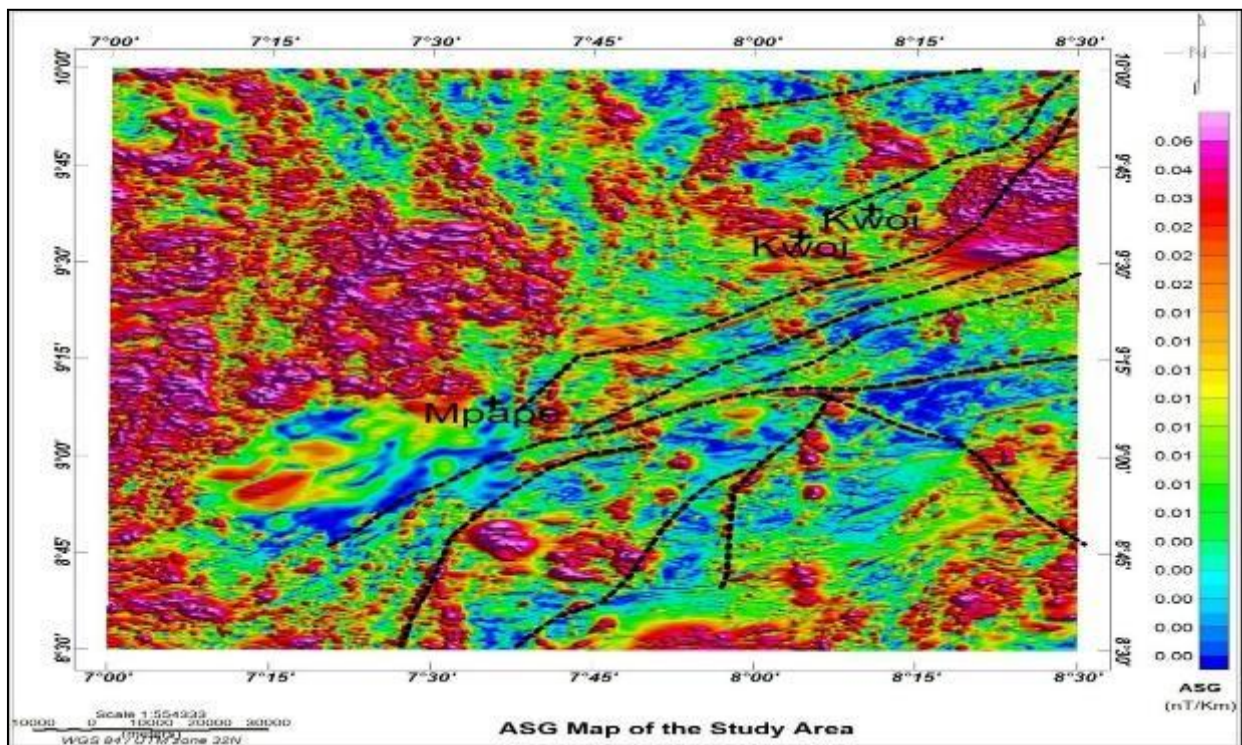


Figure 11 Analytical Signal (ASG) Map

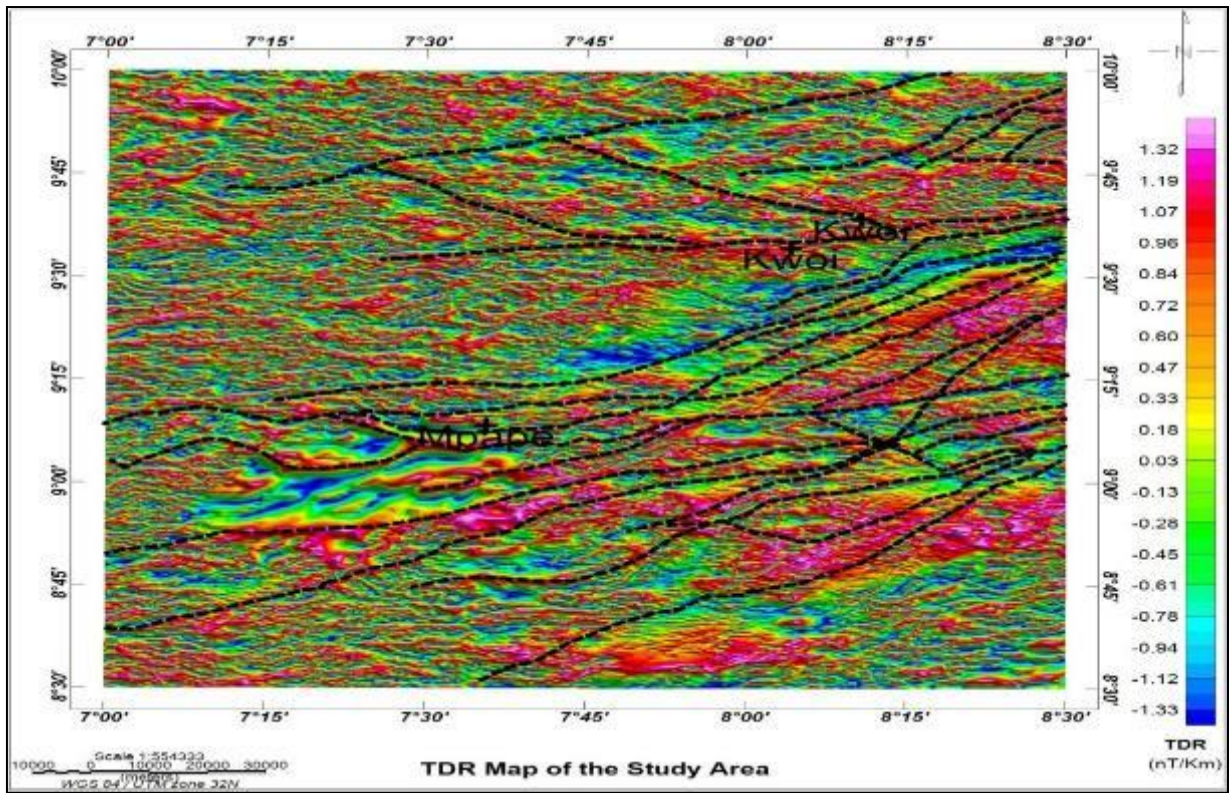


Figure 12 Tilt-angle Derivative (TDR) Map

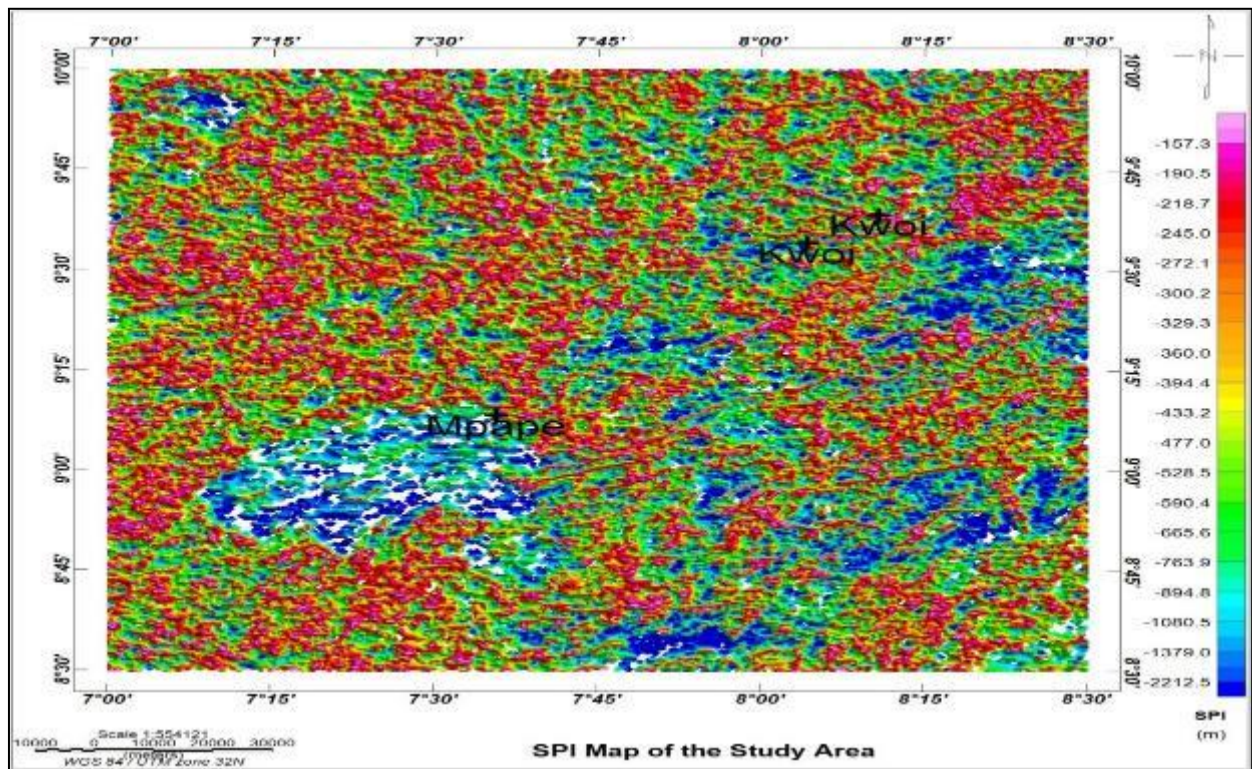


Figure 13 Source Parameter Image (SPI) Map

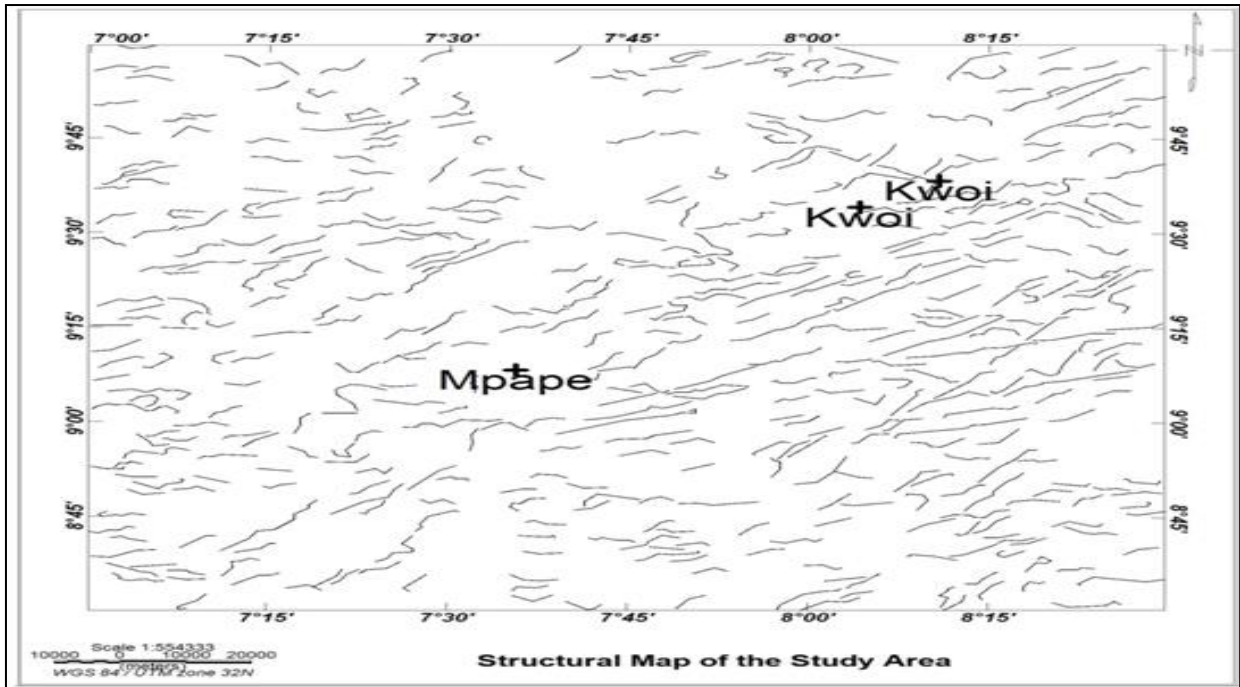


Figure 14 Aeromagnetic lineament Map

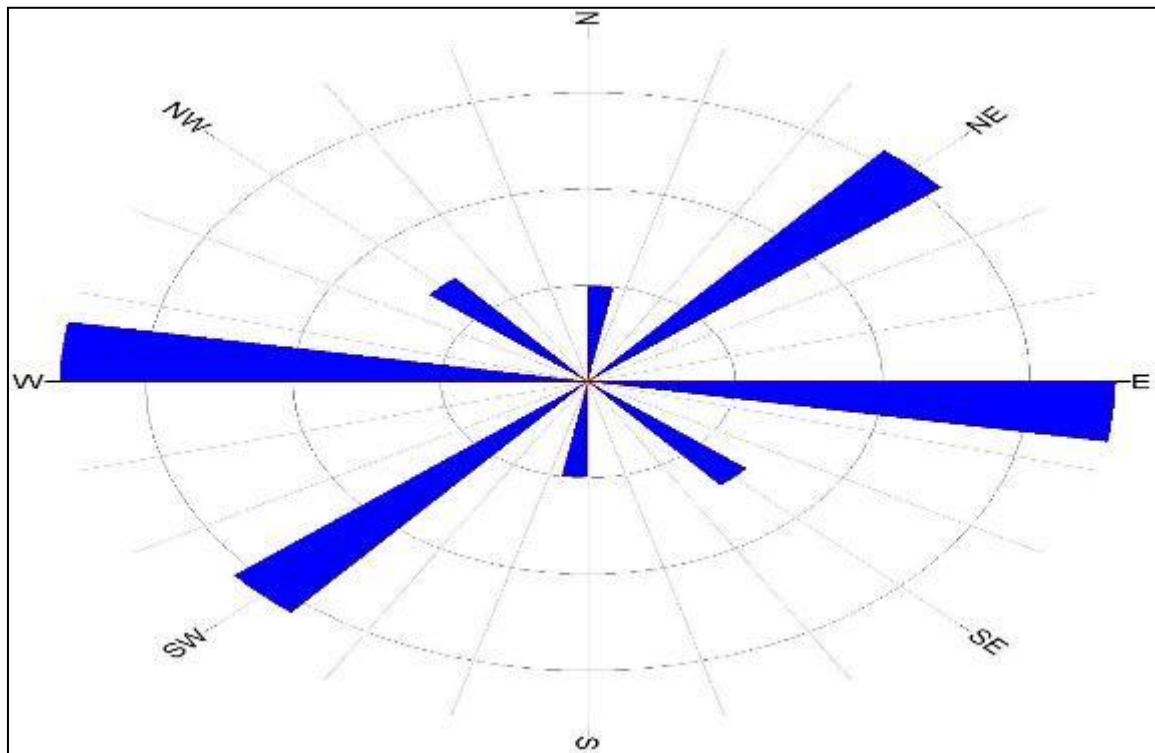


Figure 15 Rose (Azimuth-Frequency) Diagram of the Structural Map

The research area's total aeromagnetic intensity map (Figure 4) shows positive and negative anomalies ranging from -48 nT lowest to 88 nT highest, with pink to red colours indicating positive anomalies and green to blue colours indicating negative anomalies. High magnetic signature occupies Kwoi region of the research area, these anomalies could be due to presence of Biobite Granite (OGP), Granite Gneiss (GG) and undifferentiated Schists (Su). The magnetic signature

within Mpape region lies between the intermediate and high magnetic intensity, these can be due to the dominant presence of Porphyritic Granite (OGP) and Pelitic Schist (Sm).

The FVD (Figure 6) map reveals the lineament of the study location and is marked out with black lines. The anomaly gradient values on the map range from -0.5 nT/km to 0.03 nT/km. The linear magnetic structures detected on the FVD map could be from shallow or deep sources, which could be interpreted as dykes, folds, or faults, as well as boundaries or contacts separating formations. Deep structural features could be the cause of some of the anomalies in the magnetic gradient emanating from the basement. Long linear features that are continuous and less prominently trend in the NE-SW and SE-NW directions indicate lithological boundaries, which might be interpreted as major fracture or fault lines in the map passing through Mpape and Kwoi, whereas short linear and curvilinear features are observed striking NE-SW and cluster around the lithological boundaries of magnetic source bodies of Porphyritic Granite, Biotite Granite, Magmatite, Quartzite, Granite Gneiss, Medium coarse grained Biotite, Undifferentiated older Granite and Undifferentiated Schists.

The SVD map (Figure 7) indicates the presence of both high and short wavelengths, which are common, mainly along the E-W direction, and are associated to be Migmatite, porphyritic granite, granite gneiss, pelitic schist, and quartzite.

The RTE grid map was upward-continued at 1km, 2km, and 5km (Figure 8, 9, and 10). The maps recorded at various heights reveal images reflecting the magnetic intensity that will be obtained if the data are taken higher than the initial datum. Upward continuation at 1 km (Figure 8) and 2 km (Figure 9) identify two continuous linear structures cutting across the research area trending in the direction of NE-SW, one of the linear structure cuts across Mpape situated within the central region of the research area while the other cut across the northern region of the research area. These structures diminish as depth of continuation increases to 5 km (Figure 10) showing only the linear structure that cut along the Mpape region. Deep-seated basement rocks that possess high magnetic mineral constituents are found in the positive anomalous zones along the southern, eastern, western, and central regions. The upward-continuation images in showed that the dominant regional trends of the rock in the research area are striking NE-SW and E-W.

The ASG map (Figure 11) shows that the more noticeable features are the strong analytic signal in the northwestern region of the map and a small segment around the map's northeastern, southwestern, and southeastern borders, which trend NE-SW and NW-SE. There are three main categories of magnetic amplitude zones delineated: high-amplitude magnetic zones (> 0.04 nT/km), intermediate-amplitude magnetic zones (ranging from 0.01 to 0.03 nT/km), and low-amplitude magnetic zones (< 0.01 nT/km). These three varied amplitude zones are based on magnetization contrast, which is caused by varied mineralogy composition and magnetic source depth.

The TDR map (Figure 12) reveals various geological structural lineaments on the image by observing the abrupt changes between the positive and negative magnetic anomalies. The output shows major structures trending in the NE-SW and NW-SE directions.

The SPI map of the RTE-TMI (Figure 13) is characterized by shallow depths (SD), moderate depths (MD), and deeper depths (DD). The red-pink colour signifies the SD ranges from 157.3 to 300.2 m and predominantly occupies the northwestern and southwestern regions of the study area map; the green colour signifies the MD ranges from 528.5 to 763.9 m scattered all over the study area map; and the light blue-blue colour signifies the DD ranges from 894.8 to 2212.5 m identified at the Kwoi area and predominantly around the Mpape area. It is attributed to granite deposition such as Porphyritic Granite (OGp), Granite Gneiss (GG), and Migmatite (M). Also, the DD are identified around the central, southern, southwestern, and northeastern regions of the study area.

The statistical analysis of the structural trend was plotted in the form of Rose diagrams (Figure 15). An investigation of these diagrams shows two predominant sets of lineaments that are closely related to tectonic activities such as faults, fractures, and shear zones with varying intensities and lengths in the study area. The predominant tectonic trends are NE-SW and E-W, while the minor structural trends on the Rose are trending NW-SE and N-S.

Relating the lineaments to the geology, areas of high density of lineaments occur in the north-eastern region of the study area, where Kwoi is located, and the central region of the study area, where Mpape is located. The rock intrusion associated with Kwoi is Biotite Granite (MYG), while Mpape is associated with Porphyritic Granite (OGp), Granite Gneiss (GG), and Migmatite (M). Less dense lineaments occur in the northern region of the study area, with predominant rock types such as undifferentiated Schists (Su) and migmatite (M). Most high-magnitude lineaments could be attributed to deep-seated fractures, while the low-magnitude ones could be attributed to shallow weathered zones in the study area.

5. Conclusions

This study has successfully mapped the subsurface geological structures of the study area using vertical derivatives, upward continuation, source parameter imaging (SPI), tilt-angle derivative (TDR), and analytical signal (ASG), with the aim of determining the causative factors of recent seismotectonic activities in Nigeria. The results revealed the varying lithological and shallow-to-deep structure features (faults and lineaments) and their trending. The predominant tectonic trends with a high density of lineaments, which are attributed to deep-seated fractures, were observed to cut across the Kwoi and Mpape regions, which could be attributed as one of the major causes that trigger earth tremor within the basement complex.

Compliance with ethical standards

Disclosure of conflict of interest

No conflict of interest to be disclosed.

References

- [1] Adepelumi, A. A. (2019). Recent Earth Tremor in Nigeria and Its Relation to Failure of Engineering Structures: Past, Present and Future. *Journal of the Nigeria institution of Structural Engineers*, Vol. 18(2), pp. 95 – 117.
- [2] Adepelumi, A. A., Ako, B. D., Olorunfemi, J. R., Awoyemi, M. O., Falebite, D. E. (2008). Integrated Geophysical Mapping of the Ifewara Transcurrent Fault System, Nigeria. *Journal of African Earth Sciences*, Vol. 52(4-5), pp. 161-166.
- [3] Adetona, A. A., and Abu, M. (2013). Estimating the thickness of Sedimentation within Lower Benue Basin and Upper Anambra Basin, Nigeria, using both Spectral Depth Determination and Source Parameter Imaging. *Hindawi Publishing Corporation ISRN Geophysics*. Pp, 1-10.
- [4] Ajakaiye, D. E., Daniyan, M.A., Ojo, S.B., and Onuoha, K.M. (1987). The July 28, 1984 South Western Nigeria Earthquake and Its Implications for the Understanding of the Tectonic Structure of Nigeria. *Journal of Geodynamics*, Vol. 7, pp. 205-214. [http://dx.doi.org/10.1016/0264-3707\(87\)9005-6](http://dx.doi.org/10.1016/0264-3707(87)9005-6)
- [5] Ajibade, A. C., and Woakes M., (1983). Proterozoic Crustal Development in the Pan-African Regime of Nigeria. In: Kogbe, C.A., Ed., *Geology of Nigeria*, Rock View Ltd., Nigeria, pp. 57-63.
- [6] Ajibade, A.C., (1976). Proterozoic Crustal Development in the Pan-African Regime of Nigeria. In: Kogbe, C.A., Ed., *Geology of Nigeria*, Rock View Ltd., Nigeria, pp. 57-63.
- [7] Akpan, O. U., Isogun, M. A., Yakubu, T. A., Adepelumi, A. A., Okereke, C. S., Oniku, A. S., Oden, M. I. (2014). An Evaluation of the 11th September, 2009 Earthquake and its Implication for Understanding the Seismotectonics of South Western Nigeria. *Open Journal of Geology*, Vol. 4, pp. 542–550. doi:10.4236/ojg.2014.410040
- [8] Akpan, O. U., Yakubu, T. A. (2010). A Review of Earthquake Occurrences and Observations in Nigeria. *Earthq Sci*. Vol. 23(3), pp. 289–294.
- [9] Al-Badani, A. M., and Al-Wathaf, M.Y. (2018). Using the Aeromagnetic Data for Mapping the Basement Depth and Contact Locations, at Southern Part of Tihamah Region, Western Yemen. *Egyptian Journal of Petroleum* Vol. 27, pp. 485–495.
- [10] Ananaba, S. E. (1991). Dam Site and Crustal Megalineaments in Nigeria. *ITC Journal*, Vol.1, pp. 26-29.
- [11] Anifowose, A. Y. B., Oladapo, M. I., Akpan, O. U., Ologun, C. O., Adeoye-Oladapo, O. O., Tsebeje, S. Y., Yakubu, T. A. (2010). Systematic Multi-technique Mapping of the Southern Flank of Iwaraja Fault, Nigeria. *J Appl Sci Technol*, Vol. 15, pp. 70–76.
- [12] Blakely, R. J. (1995). *Potential Theory in Gravity and Magnetic Applications*, Cambridge University Press, USA, pp. 441.
- [13] Centre for Geodesy and Geodynamic (2018). *The Technical Committee Report on Abuja Seismic Tremor of 5th-7th September*.
- [14] Cooper, G. R. J. (1997) *GravMap and PFproc: Software for Filtering Geophysical Map Data*. *Computers & Geosciences*, Vol 23, pp. 91-101.

- [15] Dada, S.S. (2006). Proterozoic Evolution of Nigeria. In: Oshin, O. (ed) The Basement Complex of Nigeria and its Mineral Resources Petroc. Services Ltd. Ibadan, Nigeria. 29 – 45.
- [16] Danbatta, U. A. (2003). The Lithogeochemical Framework Underlying the Geotectonic Evolution of the Kazaure Schist Belt, Northwestern Nigeria. *The Nig J Sci Res*, Vol 4, pp. 1-13.
- [17] Danbatta, U. A. (2008). A Review of the Evolution and Tectonic Framework of the Schist Belts of Western Nigeria, West Africa. *Africa Geoscience Review*, Vol. 15(2), pp. 145-158.
- [18] Ebi, S., Nwankwo, C. N., Isogun, A. M., Afegbua, U. K., Ibitola, A. R. (2020). Determination of Compressional to Shear Wave Velocity Ratio from Local Earthquake in Nigeria between 2009-2018. *Jornal of Applied Geology and Geophysics (IOSR-JAGG)*, Vol. 8(2), pp 28-37.
- [19] Elueze, A. A. (2003). Evaluation of the 7 March 2000 Earth Tremor in Ibadan Area, South Western Nigeria. *Journal of Mining and Geology*, Vol. 39, pp. 79-83.
- [20] Eze, C. L., Sunday, V. N., Ugwu, S. A., Uko, E. D., and Ngah, S. A. (2011). Mechanical Model for Nigeria Intraplate Earth Tremors. *Articles, Disasters, Management Theme. Earth Observation, Port-Harcourt, IEEE Oceanic Engineering Society.*
- [21] Faboye, F. B., Gideon, Y. B. (2003). Improved Downward Continuation of Potential Field Data. *Exploration Geophysics*, Vol. 34, 249-256.
- [22] Feumoé, A. N., Ndougsa-Mbarga, T., Manguelle-Dicoum, E. and Fairhead, J. D. (2012). Delineation of Tectonic Lineaments Using Aeromagnetic Data for the South-East Cameroon area. *Geofizika*, Vol. 29, pp. 33-50.
- [23] Fitches, W. R., Ajibade, A. C., Egbuniwe, I. G., Holt, R. W. and Wright, J. B. (1985). Late Proterozoic Schist Belts and Plutonism in NW Nigeria. *J. Geol. Soc. London*, Vol. 142, pp. 319-337.
- [24] Gunn, P.J. (1975). Linear Transformation of Gravity and Magnetic Fields. *Geophysical Prospecting*, Vol. 23, pp. 300-312. <https://doi.org/10.1111/j.1365-2478.1975.tb01530.x>
- [25] Hsu, N. C., Herman, J. R., Bhartia, P. K., Seftor, C. J., Torres, O., Thompson, A. M., Gleason, J. F., Eck, T. F., and Holben, B. N., (1996). Detection of Biomass Burning Smoke From TOMS Measurements. *Geophysics. Res. Lett.*, Vol. 23, pp. 745–748.
- [26] Isogun, A. M., Afegbua, U. K., Nuhu T. A., and Abba J. M. (2018). The Compressional to Shear Wave Velocity Ratio of the Crust and Uppermost Mantle of Nigeria. *International Journal of Science Engineering and Research (IJSER)*, Vol. 5(157) pp 142-147.
- [27] Kroner, A., Ekweme, B. N. and Pidgeon, R.T. (2001). The Oldest Rock in West Africa: SHRIMP Zircon Age for Early Archaean Migmatitic Orthogneiss at Kaduna, Northern Nigeria. *Journal of Geology*, Vol. 109(3), pp. 399-406.
- [28] McCurry, P. (1976). The geology of the Precambrian to lower Paleozoic rocks of Nigeria. In: Kogbe, C.A. (ed) *Geology of Nigeria*. Elizaberthan, Lagos, Nigeria. 15-31.
- [29] Mekonnen, T. K. (2004). Interpretation and Geodatabase of Dykes Using Aeromagnetic Data of Zimbabwe and Mozambique, M.Sc. Thesis, ITC, Delft, the Netherlands.
- [30] Murat, R. C. (1988). Airphoto Interpretation as an aid to Litho –Structural Mapping Intropical Terrain: The New Federal Capital City Site, Abuja, Nigeria. *Mineral Resources Exploration. Bulletin*, Vol. 108, pp. 65 -75.
- [31] Nabighian, M. N. (1972). The Analytic Signal of Two Dimensional Magnetic Bodies With Polygonal Cross Section: Its Properties And Use for Automated Anomaly Interpretation. *Geopgysics*. Vol. 37(2), pp. 507-517.
- [32] Nabighian, M. N. (1984): Towards the Three-Dimensional Automatic interpretation of Potential Field Data via Generalised Hilbert Transforms: Fundamental Relations. *Geophysics*, Vol. 53, pp. 957-966.
- [33] Nathaniel, G. G., Solomon, A. O., Adama, B. O., Shekwoyandu, I., Ishak, Y. T., Aisha, A. K., Allu A.U., and Halima, O. U. (2020). Preliminary Geological Evidence for Multiple Tremors in Kwoi, Central Nigeria. *Journal of Geoenvironment Disasters*, Vol. 7(22).
- [34] Nwankwoala, H. O. and Orji, O. M. (2018). An Overview of Earthquakes and Tremor in Nigeria: Occurrences, Distributions and Implications for Monitoring. *International Journal of Geology and Earth Sciences*, Vol. 4(2), pp. 56-76. [Doi:10.32937/IJGES.4.4.2018.56-76](https://doi.org/10.32937/IJGES.4.4.2018.56-76).
- [35] Obaje, N. G. (2009). *Geology and Mineral Resources of Nigeria*. Berlin: Springer-Verlag, Heidelberg, pp. 221.

- [36] Obiora, S. C. (2005). *Field Descriptions of Hard Rocks with Examples from the Nigerian Basement Complex* (1st Edition). Snap Press (Nig.) Ltd. Enugu, 14.
- [37] Ojo, O. M. (1995). Survey of Occurrences in Nigeria of Natural and Man-Made Hazards Related to Geological Processes. In: Onuoha, K.M. and Offodile, M.E., Eds., *Proceedings of the International Workshop on Natural and Man-Made Hazard in Africa*, Nigeria Mining and Geosciences Society Publication, Jos, pp. 10-14.
- [38] Ojoh, K. (1992). The Southern part of the Benue Trough Nigeria Cretaceous Stratigraphy, Basin Analysis, Paleoceanography and Geodynamic evolution in the Equatorial Domain of the South Atlantic. *NAPE Bulletin* 7, Pp. 131-152.
- [39] Oluwafemi, J.O., Ofuyatan, O.M., Ede, A. N., Oyebisi, S.O., & Akinwumi, I. I. (2018). *International Journal of Civil Engineering and Technology (IJCIET)*, Vol. 9(8), pp 1023-1033.
- [40] Onuoha, K. M. (1988). Earthquake Hazard Prevention and Mitigation in the West Africa Sub-Region. *Natural and Man-made Hazards*, pp. 787-797.
- [41] Osagie, E. O. (2008). Seismic Activity in Nigeria. *The Pacific Journal of Science and Technology*, Vol 9, pp. 1-6.
- [42] Oyawoye, M. O. (1964). The Geology of the Nigerian Basement Complex – A survey of our present Knowledge of them. *J. Niger. Min. Geol. Metall. Soc.*, Vol. 1, pp. 87-103.
- [43] Oyawoye, M. O. (1965). Review of Nigerian Pre-cretaceous. In: Reymont, R. A., *Aspect of the Geology of Nigeria*, University of Ibadan Press, pp. 16-21.
- [44] Oyawoye, M. O. (1972). The Basement Complex of Nigeria. In Dessauvague, T. F., and Whiteman, A. J., eds. *African geology*. Ibadan, Geology Department, University of Ibadan, pp. 42-98.
- [45] Oyibo, D., Omali, A. O., Kadiri, U. A., Iduma, K. U. (2022). Geophysical Evaluation of Central Nigeria Earth Tremor Activities using High Resolution Airborne Magnetic Data. *Journal of Advances in Research*, Vol. 23(2), pp. 23-38.
- [46] Rahaman, M. A. (1988). Recent Advances in the Study of the Basement Complex of Nigeria. In: *Precambrian Geology of Nigeria*, (Eds. Oluyide et al.) a publication of the Geological Survey of Nigeria, pp. 11-43.
- [47] Roest, W. R., Verhoef, J. and Pikington, M. (1992). Magnetic interpretation using the 3-D analytic signal. *Geophysics*, 57: 116-125.
- [48] Salako, A. K. (2014). Depth to Basement Determination Using Source Parameter Imaging (SPI) of Aeromagnetic Data: An Application to Upper Benue Trough and Borno Basin, Northeast, Nigeria. *Academic Research International*, Vol. 5(3).
- [49] Sykes, L. R. (1978). Intraplate Seismicity, Reactivation of Preexisting Zones of Weakness, Alkaline Magmatism, and Other Tectonism Postdating Continental Fragmentation, *Rev. Geophys.*, Vol. 16, pp. 621-688.
- [50] Telford, W. M., Geldart, L. P., & Sheriff, R. E. (1990). *Applied Geophysics*, Cambridge: Cambridge University Press, pp. 64-84.
- [51] Thurston, J. B., and Smith, R. S. (1997). Automatic Conversion of Magnetic Data to Depth, Dip and Susceptibility Contrast Using the SPITM Method. *Geophysics*, Vol. 62, pp. 807-813.
- [52] Tsalha, M. S., Lar, U. A., Yakubu, T. A., Umar, A. K., and Duncan D. (2015). The Review of the Historical and Recent Seismic Activity in Nigeria. *IOSR, Journal of Applied Geology and Geophysics*, Vol.3(1), pp. 48-56.e-ISSN; 2321-0990.
- [53] Umeaku, O. C. and Emujakporue, G. O. (2020). Evaluation of Aeromagnetic Data for Delineation of Geological Structures in Earth Tremor Area in Part of Kaduna State, Nigeria. *Journal of Science and Technology*, Vol. 6(21).
- [54] Wright, J. B., Hastings, D. A., Jones, W. B., Williams, H. R. (1985). *Geology and Mineral Resources of West Africa*. Allen and Urwin, London pp.187.